Biosensors and Bioelectronics 66 (2015) 162–168

Contents lists available at ScienceDirect

Biosensors and Bioelectronics

journal homepage: www.elsevier.com/locate/bios

Self-powered microneedle-based biosensors for pain-free high-accuracy measurement of glycaemia in interstitial fluid

L.M. Strambini [a], A. Longo [a], S. Scarano [b], T. Prescimone [c], I. Palchetti [b], M. Minunni [b], D. Giannessi [c], G. Barillaro [a,c,*]

[a] Dipartimento di Ingegneria dell'Informazione, Università di Pisa, via G. Caruso 16, 56122 Pisa, Italy
[b] Dipartimento di Chimica 'Ugo Schiff', Università di Firenze, via della Lastruccia 3, 50019 Sesto Fiorentino, Italy
[c] Istituto di Fisiologia Clinica, Consiglio Nazionale delle Ricerche (CNR), via G. Moruzzi, 1, 56124 Pisa, Italy

ARTICLE INFO

Article history:
Received 1 September 2014
Received in revised form
22 October 2014
Accepted 6 November 2014
Available online 10 November 2014

Keywords:
Microneedles
Biosensors
Glycaemia
Diabetes
Pain-free

ABSTRACT

In this work a novel self-powered microneedle-based transdermal biosensor for pain-free high-accuracy real-time measurement of glycaemia in interstitial fluid (ISF) is reported.

The proposed transdermal biosensor makes use of an array of silicon-dioxide hollow microneedles that are about one order of magnitude both smaller (borehole down to 4 μm) and more densely-packed (up to 1×10^6 needles/cm^2) than state-of-the-art microneedles used for biosensing so far. This allows self-powered (i.e. pump-free) uptake of ISF to be carried out with high efficacy and reliability in a few seconds (uptake rate up to 1 μl/s) by exploiting capillarity in the microneedles. By coupling the microneedles operating under capillary-action with an enzymatic glucose biosensor integrated on the backside of the needle-chip, glucose measurements are performed with high accuracy ($\pm$20% of the actual glucose level for 96% of measures) and reproducibility (coefficient of variation 8.56%) in real-time (30 s) over the range 0–630 mg/dl, thus significantly improving microneedle-based biosensor performance with respect to the state-of-the-art.

1. Introduction

According to estimation of the International Diabetes Federation (IDF) 382 million people worldwide have diabetes (IDF Diabetes Atlas, 2013). IDF projects that people living with diabetes will be 592 million in 2035. A number of recent studies clearly indicated that implementing strict glycaemic control can effectively reduce the risk of serious complications (American Diabetes Association, 2010) in diabetic patients (DPs) and, in turn, deaths (UK Prospective Diabetes Study (UKPDS) Group, 1998; Holman et al., 2008; The Diabetes Control and Complications Trial Research Group, 1993; Nathan et al., 2005; Kitzmiller et al., 2008).

Long-term, accurate sensing of blood glucose concentration is a major concern for diabetic patients (Gilligan et al., 2004), and satisfactory compliance with testing is difficult to achieve, given the painful repetitive nature of the commonly used finger-prick systems available on the market (Martin et al., 2006; Shlomowitz and Feher, 2014). It has been recently shown that interstitial fluid (ISF) glucose concentrations parallel those of blood glucose (Stout et al., 2001; Vesper et al., 2006). Subcutaneously-implanted systems working on ISF and allowing for continuous glucose monitoring up to one week have then come to market in the effort to alleviate discomfort by repeated injections (Tamborlane et al., 2008; Lodwig et al., 2014). Nonetheless, these systems make use of catheters that must be inserted in the subcutaneous tissue and replaced intermittently.

Microneedles systems emerged in the mid-1990s as a result of progress in micro- and nano-technologies. They have been demonstrated to be pain-free and potentially low-cost and easy-to-use (Kim et al., 2012; El-Laboudi et al., 2013). Over the last decade they have been widely used for the transdermal delivery of a number of drugs and compounds (insulin, proteins, DNA, vaccines, and others) (Kim et al., 2012), but only a few studies have been reported on their use for glucose measurements by either extraction of biological fluid and successive analysis or in-situ analysis (Kim et al., 2012; El-Laboudi et al., 2013). Microneedles targeting ISF are particularly appealing, with respect to those sampling blood, for their unique characteristic of being pain-free and blood-free (Kim et al., 2012; El-Laboudi et al., 2013).

The analysis of the state-of-the-art on the use of microneedles for glucose measurements in ISF underlines how chips containing a reduced number of needles, ranging from 1 to 300, with length from 200 to 1500 μm and tip radii from 15 to 400 μm have been

* Corresponding author at: Dipartimento di Ingegneria dell'Informazione, Università di Pisa, via G. Caruso 16, 56122 Pisa, Italy. Fax: +39 050 2217 522.
E-mail address: g.barillaro@iet.unipi.it (G. Barillaro).

http://dx.doi.org/10.1016/j.bios.2014.11.010
0956-5663/

proposed for ISF extraction and subsequent glucose concentration measurement (Mukerjee et al., 2004; Wang et al., 2005; Sakaguchi et al., 2012; Zimmermann et al., 2003). However, in most of this works the needles are only used to pierce the skin, whereas collection of ISF is carried out using either vacuum pumps or hydrogel patches, and measurements of the glucose concentration is performed off-line by using standard analytical equipments (Mukerjee et al., 2004; Wang et al., 2005; Sakaguchi et al., 2012). To the best of our knowledge, only two works report the use of microneedles for real-time glucose measurements in ISF (Zimmermann et al., 2003; Miller et al., 2012). Nonetheless, in (Zimmermann et al., 2003) ISF is pumped with a flow-rate of 100 μl/min through an integrated enzyme-based glucose sensor for in-line glucose measurement and the sensor linearity range is limited to 0–160 mg/dl; in (Miller et al., 2012) hollow polymer microneedles with borehole of 400 μm and length of 1500 μm are filled with enzyme-enriched carbon paste material and used for in-situ glucose detection in the range 0–216 mg/dl, but no ISF uptake through the needles is carried out.

In this work we make use of hollow silicon-dioxide microneedles that are up to one order of magnitude both smaller (needle borehole with diameter of 4 μm) and more densely-packed (1×10^6 needles/cm^2) than those commonly used for biosensing. We demonstrate for the first time that, by exploiting capillarity in such microneedles, accurate, reproducible, and fast uptake of liquids (e.g. water, standard physiological solution, ISF) is achieved, without the need of using external pumps. We show that, by coupling such microneedles operating under capillary-action with an enzymatic glucose biosensor integrated on the back-side of the needle-chip, self-powered real-time measurement (in-vitro) of glucose concentration in ISF is carried out with high accuracy, high reproducibility, and excellent linearity over the range 0–630 mg/dl.

2. Materials and methods

2.1. Microneedle chip: design and fabrication

Fabrication of the microneedle chips is carried out by (1) microneedle integration, on the front-side of a silicon die, and (2) reservoir integration, on the back-side of the same silicon die, as detailed in (Strambini et al., 2012). The needles protrude from the front-side of the chip and are in connection, through an internal channel, with the reservoir grooved on the back-side of the chip.

Two different types of microneedle chips are fabricated and tested, both of which integrating, over an area of 0.5 cm × 0.5 cm, needles with same silicon-dioxide thickness (about 1 μm) and same protruding length (about 100 μm), but different pitch p, external diameter d_e, and internal diameter d_i. In particular, type#1 microneedle chips are characterized by pitch $p=16$ μm (density 6.25×10^5 needles/cm^2), external diameter $d_e=9$ μm, and internal diameter $d_i=7$ μm; type#2 microneedle chips are characterized by pitch $p=10$ μm (density 1×10^6 needles/cm^2), external diameter $d_e=6$ μm, and internal diameter $d_i=4$ μm. In both cases, the internal channel of the needles has length $l=200$ μm and allows fluidic connection of the needles with the trapezoidal-shaped reservoir grooved on the back-side of the chips. Size and depth of the reservoir are 0.5 cm × 0.5 cm and 500 μm, respectively (geometrical volume 10 μl) for chips used in experiments aimed at demonstrating self-powered uptake of interstitial fluid using microneedles operating under capillary-action; 0.70 cm × 0.57 cm and 500 μm (geometrical volume of about 18 μl) for chips used in experiments aimed at demonstrating in-vitro glucose measurement in interstitial fluid using microneedles operating under capillary-action.

2.2. Testing solutions: preparation and titration

Synthetic ISF solutions containing 11 g/l of total proteins are prepared by dissolving human albumin (fraction V) and α-globulins (Cohn fraction IV-1) (both supplied by Sigma-Aldrich) in a ratio 60:40 in standard physiological solution (PSS) (0.9% NaCl) containing 6 mg/l of ProClin 150 (Supelco-Sigma-Aldrich) as preservative (Fogh-Andersen et al., 1995; Collison et al., 1999).

Standard solutions containing known amount of glucose are prepared starting from a 1 M stock solution of D(+) glucose (Sigma-Aldrich) in ISF and in phosphate saline buffer (PBS). Eight glucose calibrators in the physiopathological range (0–35 mM corresponding to 0–630 mg/dl) are obtained both in ISF and in PBS. In order to check possible matrix effects and as a overall control of the calibrator preparation, glucose concentration of all the calibrators are measured in triplicate by AU400 platform by Beckman Coulter using an enzymatic hexokinase method. This system provides a linear response between 0 and 45 mM (from 0 to 800 mg/dl). Sensitivity, which is evaluated as mean value plus 3x standard deviations of 20 repeated measurements of glucose-free samples, is 0.04 mM (0.72 mg/dl). Both for ISF and PBS solutions the mean within-run variation relative to three replicate measures is $<0.5\%$ at all the glucose concentrations. Total protein concentration in the ISF solution is also confirmed by AU400 system measure. Glucose is undetectable in the ISF solution at baseline (before addition of known glucose amount), indicating the lack of interference effects due to the matrix on glucose measure by hexokinase method on Beckman−Coulter system. For all the different glucose calibrators, both in ISF and PBS, a quantitative recovery of the added glucose is achieved. Glucose measure is free from significant media effects, as demonstrated by the linearity of the response (glucose measured vs. glucose added) and by the intercept values not significantly different from zero (for the ISF solution $y=1.04x-3.14$; $R^2=0.997$).

Density and dynamic viscosity of PSS and ISF solution are measured using standard pycnometer and U-tube viscosimeter, respectively, using deionized water (DIW) as reference. Contact angle of DIW, PSS, and ISF solution with silicon dioxide is measured by standard static sessile drop method on a flat oxide surface, obtained by dry thermal oxidation of silicon and chemically modified with Piranha solution (sulfuric acid, H_2SO_4 95–98% in water, and hydrogen peroxide, H_2O_2 30% in water, 3:1 by volume).

2.3. Fluid drawing by capillary-action with microneedles: measure protocol

A known volume (10 ml) of the liquid under test is placed into a glass Petri dish positioned on top of an analytical microbalance (accuracy 0.1 mg) that allows monitoring volume changes of the liquid substance over time by measuring weight losses, which are mainly due, in our experiments, to microneedle uptake by capillary-action and to evaporation by free-convection (unwanted effect). The microneedle chip, with the needles pointing downward, is brought in contact with the liquid through the use of a micropositioner so as to submerge the needles into the liquid for their entire protruding length, thus mimicking insertion of the needles into skin in real-word operation. As soon as the needles are immersed in the liquid, the volume, and in turn the weight, of the liquid in the Petri dish reduces due to uptake through the needles by capillary action until the reservoir of the chip is completely filled, as well as to free-convection evaporation over time. For each tested liquid at least six measurements are carried out over a time span of 900 s, for both type#1 and type#2 chips, at room

temperature. Quantification of free-convection evaporation is carried out for each single measure by performing the linear regression of experimental data in the range 300–900 s, for which weight reduction is linear and only due to evaporation. The slope of the regression line ($R^2 > 0.999$ for any experimental measurement) gives the evaporation rate, which is used to eliminate evaporation effects and to only retain capillary-uptake effects.

After each single measurement, the chip is cleaned according to the following procedure: rinsing in deionized water for 10 min, cleaning in Piranha solution for 15 min to remove possible organic components, rinsing in deionized water for 10 min and with ethanol for 1 min, and eventually nitrogen flow drying. Before and after any set of measurements with a specific liquid, six control measurements in DIW are carried out to check possible either partial or total occlusion of the needles upon testing. The whole measurement protocol is repeated several times in order to investigate reliability of liquid uptake by capillary-action through the microneedles.

2.4. Screen-printed glucose biosensor: design and preparation

Biosensor electrodes are screen-printed using a DEK 248 machine (DEK, Weymouth, UK), using both carbon-based polymeric ink (Electrodag 423 SS, from Acheson, UK) and insulating ink (TCI8700, from Visprox BV, The Netherlands). A polyester flexible foil (Autostat CT5, from MacDermid Autotype Ltd., UK), is used as the printing substrate. The carbon ink is used to define counter and working electrodes, as well as contact leads on the polyester foil, then curing at 120 °C for 10 min of the printed carbon layer is performed. The insulating ink is used to partially cover the electrode surfaces so as to define the electrode working area (7 mm^2), as well as to cover unnecessary part of the contact leads. Curing of the printed insulating layer is then performed at 70 °C for 20 min. The electrodes are modified using an enzyme layer consisting of a hydrophilic polymer (carboxymethylcellulose (CMC), Sigma-Aldrich), an oxidoreductase (Glucose oxidase (GOD), from *Aspergillus niger*, Type II-S, Sigma-Aldrich), and an electron acceptor ($K_3[Fe(CN)_6]$, Sigma Aldrich). In particular, 5 μL of a solution containing 1% CMC, 2 U/electrode of GOD, and 100 mM Ferricyanide in 0.1 M PBS is cast over the whole electrode working area, then dried in a warm air drier (40 °C for 10 min). Eventually, electrodes are bagged, sealed, and stored at 4 °C until use.

2.5. Microneedle-based biosensors: architecture and measure protocol

For the realization of microneedle-based biosensors for real-time measurement of glucose in ISF samples collected by capillary-action through the needles, both type#1 and type#2 chips are coupled with the screen-printed graphite electrodes modified with glucose-oxidase enzyme, which is inserted in the reservoir of the chip for a depth of 300 μm, thus reducing the reservoir volume to 5 μl in operating condition.

A volume of 5 μl of the solution under test is drained through the microneedles by capillary-action into the reservoir so as to completely fill the detection chamber and, in turn, get in contact with the active area of the glucose biosensor. A wait-time of 5 s and 35 s after the needles are brought in contact with the solution under test is applied for type#1 and type#2 chips, respectively, before biasing the glucose biosensor. Chrono-amperometric measurements are performed using an applied potential of +0.5 V (vs. pseudo-reference electrode). This value is optimized by both cyclic voltammetry and chrono-amperometry. Current recorded at such a potential value is due to potassium ferrocyanide (i.e. the mediator) oxidation and corresponds to glucose concentration, according to the reaction mechanism occurring in "second generation" (mediator-based) glucose biosensors (Wang, 2008). Analytical parameters are calculated for different sampling times, from 5 to 200 s, over the whole range of glucose concentrations, from 0 to 35 mM. All measurements are performed at room temperature and without degassing the samples.

2.6. Analytical parameters: definition and calculation

Accuracy A is evaluated by calculating errors between measured and actual glucose concentrations, that is $A = C_m - C_a = (I_m - I_a)/S$, where C_m and C_a are the measured and actual glucose concentrations, respectively, I_m and I_a are the measured and ideal sensor current values, respectively, for the specific glucose concentration C_a, and S is the sensor sensitivity.

Linearity is evaluated as the squared correlation coefficient R^2 of the linear regression curve best-fitting I_m–C_a experimental data.

Reproducibility is evaluated by calculating the coefficient of variation $\%CV = \sigma/\mu \times 100$ of the sensor current I_m for each glucose concentration C_a, being σ the standard deviation and μ the mean value of I_m, then averaging the calculated %CV values over the whole range of glucose concentrations and achieving an average %CV ($\%CV_{av}$).

Sensitivity S is evaluated from the slope of the linear regression curve best-fitting I_m–C_a experimental data.

Resolution is evaluated by calculating the limit-of-detection $LoD = 3\sigma/S$, being σ the standard deviation value of the sensor current I_m for the tested solution at zero-glucose concentration.

All the analytical parameters are calculated for each sampling time, over the whole range of tested glucose concentrations.

3. Results and discussions

3.1. Self-powered uptake of interstitial fluid using microneedles operating under capillary-action

The microneedle chip of this work is sketched in Fig. 1a and consists of a silicon die featuring a two-dimensional array of hollow silicon-dioxide needles protruding from the front-side of the chip for one hundred microns, in connection with a reservoir integrated on the back-side of the chip. Two different types of microneedle chips are fabricated and tested, namely type#1 and type#2, featuring needles with different period/density and external/internal diameter, but same reservoir, as detailed in Section 2.1. Scanning Electron Microscope (SEM) images at two different magnifications of type#1 microneedles are reported in Fig. 1c and d, with a typical insulin needle sitting on their top for comparison. SEM images at two different magnifications of a part of the reservoir integrated on the back-side of the same chip are shown in Fig. S1a and S1b (Supplementary materials).

Both type#1 and type#2 microneedle chips (Fig. 2a) are used to investigate and quantify the ability of such tiny and dense needles to collect liquid substances efficiently into the reservoir integrated on the back-side by exploiting capillary action, once the needles are immersed into a liquid for a depth equal to their protruding length, thus mimicking insertion of the needles into tissues.

Three different liquid solutions are taken into account for the tests: (i) deionized water (DIW), which is used as control solution, (ii) standard physiological solution (PSS) and (iii) interstitial fluid (ISF), which are of clinical interest. The ISF is a synthetic surrogate solution mimicking in-vivo ISF and containing a concentration of 11 g/l of protein obtained by solubilizing in the ratio 60:40 human albumin and α-globulins in standard physiological solution, prepared as detailed in Section 2.

Typical time-resolved liquid-uptake curves of DIW, PSS, and ISF obtained for both type#1 and type#2 microneedle chips operating

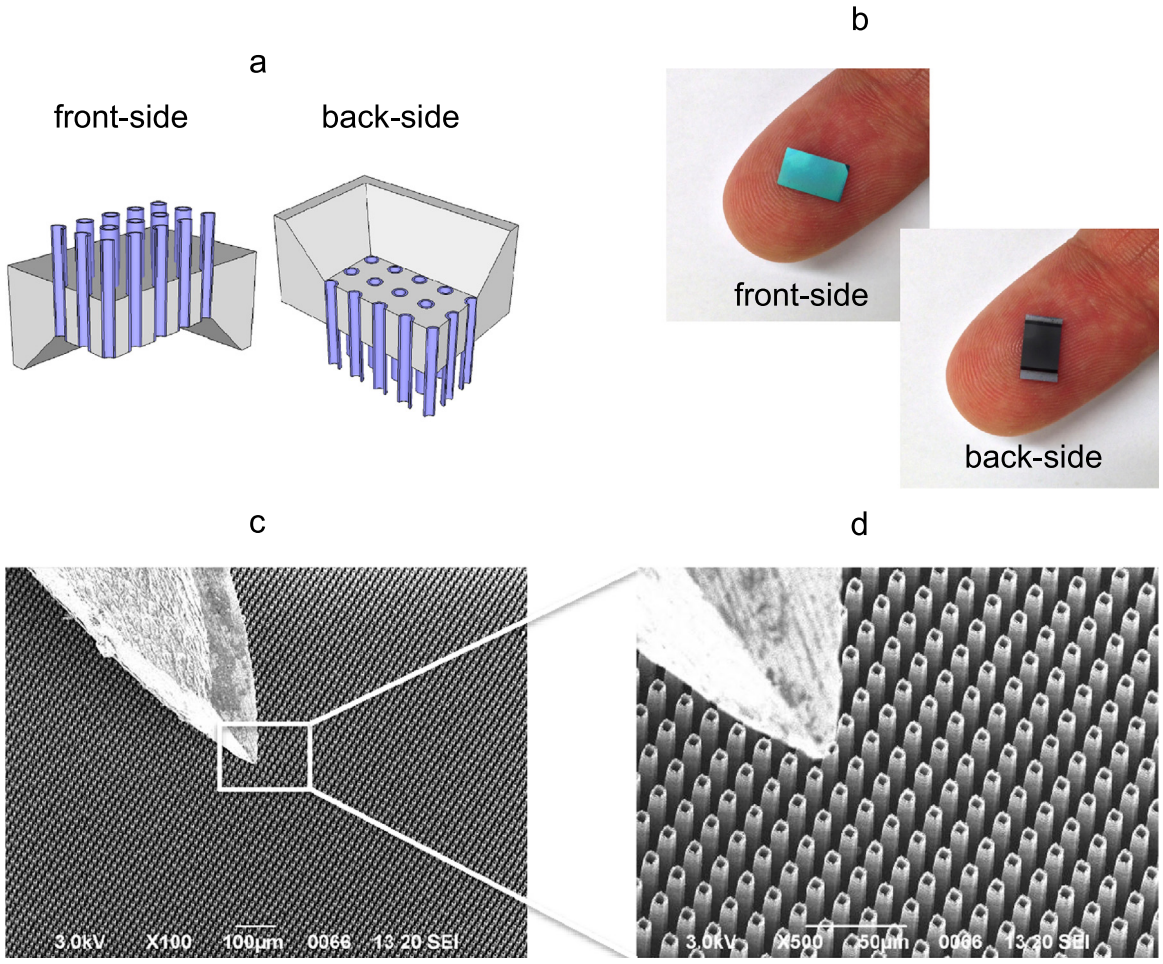

Fig. 1. High-density out-of-plane microneedle chip. (a) Schematic of a part of the microneedle chip used in this work highlighting the array of hollow silicon-dioxide needles protruding from the front-side surface and in connection with the reservoir integrated on the back-side of the chip. (b) Optical image of a type#1 microneedle chip on top of a finger. (c) and (d) Bird-eye-view scanning electron microscope (SEM) images at two different magnifications of type#1 microneedles with a typical insulin needle sitting on their top for comparison.

under capillary-action are shown in Fig. 2b. The curves are properly corrected from free-convection evaporation of the liquid over time at room temperature under atmospheric pressure, as shown in Fig. S1c (Supplementary materials), according to the procedure detailed in Section 2. It is apparent that type#1 needles are significantly faster (a factor 10 for ISF) than type#2 needles for any tested liquid. For both the microneedle chips and independently of the liquid under test, time-resolved liquid-uptake curves feature a first-order-system kinetics $V(t)=V_\infty(1-e^{-t/\tau})$, being $V(t)$ the volume of liquid in the reservoir over time and V_∞ its steady-state value, which is measured to be 17 ± 1 µl for all the tested liquids and mainly depends on the reservoir geometric features, and τ the characteristic time-constant of the system, which depends on both microneedle size and density as well as on the specific liquid under test (namely, τ is about 12.4 s and 110.7 s for ISF uptaking using type#1 and type#2 needles, respectively). Fig. 2c shows the characteristic time-constant τ (mean value and standard deviation) for the three tested liquids, both for type#1 and type#2 chips, obtained through best-fitting of experimental data with a first-order-system kinetics curve ($R^2>0.998$). The liquid uptake dynamics is mainly determined by a balance between capillary pressure, which drives the liquid throughout the needles, and viscous losses of the liquid at the needle internal surface, which act as a dissipation factor. Contact angle of the liquid at the needle internal surface, dynamic viscosity of the liquid, radius, length, and period of the needles, width and height of the reservoir in contact with the needles will all play a role on the capillary uptake of liquids, accordingly to capillary-microfluidics theory (Joos, 1999). The liquid uptake-rate (UR) through the microneedle chips can be calculated by taking the first derivative of time-resolved liquid-uptake curves, that is $UR=dV(t)/dt$, which yields $UR=(V_\infty/\tau)e^{-t/\tau}$ and highlights as the uptake-rate has an initial maximum value $UR_0=V_\infty/\tau$ (at $t=0$) and monotonically reduces (down to zero at $t=\infty$) as the uptake time (drained volume) increases. For ISF uptaking, the maximum uptake-rate value UR_0 is about 1.37 µl/min and 0.15 µl/min using type#1 and type#2 needles, respectively.

Control measurements in DIW are carried out before and after tests with PSS and ISF, and confirm that experiments and results of liquid-uptake by capillary-action are not affected by significant artifacts, independently of the liquid under test and of the type of chip (Fig. 2d). For both type#1 and type#2 chips, time-constant and, in turn, the time needed to fill the reservoir, increases from DIW to PSS and ISF. This can be explained in terms of different properties, e.g. surface tension, viscosity and density, of the tested liquids (Table S1 in Supplementary materials). Experimental evaluation of the time required to uptake a volume of 5 µl of ISF, in which quantify glucose with type#1 and type#2 chips, results in about 5 s and 35 s for type#1 and type#2 chips, respectively (Fig. S1d in Supplementary materials).

It has to be noted that for both type#1 and type#2 chips high accuracy and good reproducibility of the capillary-uptake process is achieved for all the tested liquids, as it is apparent from the

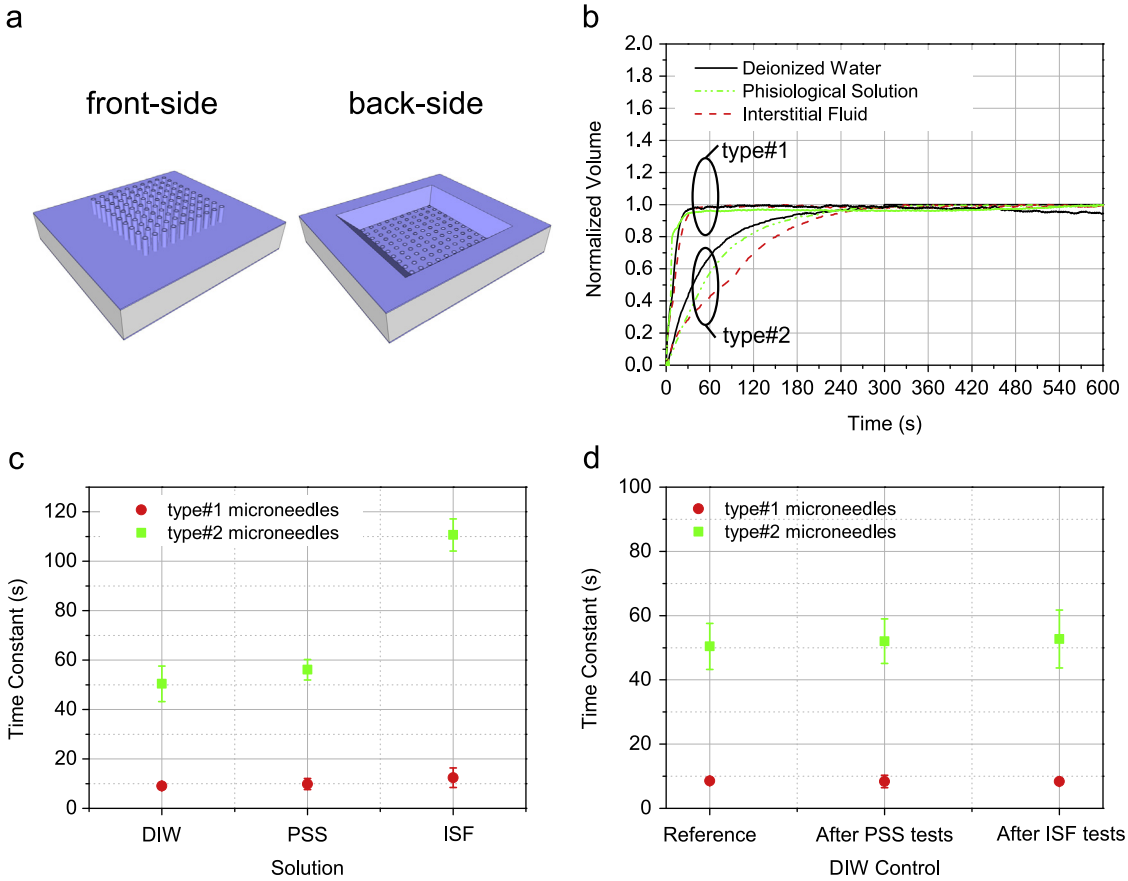

Fig. 2. Capillary (pump-free) uptake of interstitial fluid with hollow microneedles. (a) Schematic – front-side and back-side – of the chip used for capillary uptake of liquids with hollow microneedles. (b) Typical time-resolved curves for uptake of DIW, PSS, and ISF by capillary-action using type#1 and type#2 microneedles. (c) Characteristic time-constant τ (mean value and standard deviation) for uptake of DIW, PSS, and ISF by capillary-action with type#1 and type#2 microneedles. (d) Control measurements in DIW of liquid-uptake by capillary-action using type#1 and type#2 microneedles.

small standard deviation of the performed measurements. On the one hand, the very small borehole of the needles allows to significantly increase capillary force and, in turn, to improve efficiency and accuracy in liquid collection. On the other hand, the very high needle density allows to effectively address possible occlusion of some needles within the array and, in turn, to improve reproducibility and uptake-rate in liquid collection.

3.2. In-vitro glucose measurement in interstitial fluid using microneedles operating under capillary-action

Both type#1 and type#2 chips are used for the realization of microneedle-based transdermal biosensors for real-time measurement of glucose in ISF samples (volume of 5 μl) collected by capillary-action through the needles. To this end, the reservoir integrated on the back-side of the chips is slightly modified as in Fig. 3a-1 to allow coupling of the microneedles (Fig. 3a-2) with a glucose biosensor (Fig. 3a-3), this latter consisting of screen-printed graphite electrodes modified with glucose-oxidase enzyme. The trapezoidal-shaped reservoir has size of 0.70 cm × 0.57 cm and depth of 500 μm (geometrical volume of about 18 μl). This value reduces to 5 μl in operating condition, that is after coupling of the microneedle chip with the glucose biosensor, which is inserted in the reservoir for a depth of 300 μm. Optimization of the analytical performance of the glucose biosensor is out of the scope of this work and attainable, if necessary, by using a more sophisticated surface chemistry (Jang et al., 2012; Chen et al., 2013; Yang et al., 2014; Hsu and Wang, 2014; Taguchi et al., 2014) that could be exploited to improve analytical performance of the microneedle-based biosensor.

The microneedle-based glucose biosensors (Fig. 3a-4) are characterized using glucose solutions, both in ISF (which is a complex matrix) and in PBS (as control solution), with different concentrations in the range 0–35 mM (0–630 mg/dl), which is of clinical interest for diabetes. Preparation, titration, and characterization of all the tested solutions are detailed in Section 2. A volume of 5 μl of the solution under test is drained through the microneedles by capillary-action so as to completely fill the detection chamber at open circuit potential. This is achieved by applying a wait-time of 5 s for type#1 chips and 35 s for type#2 chips, after the needles are brought in contact with the solution and before biasing the biosensor, according to the time required to uptake 5 μl of ISF (which has the slowest uptake-rate) by capillary-action using the microneedles (Fig. S1d). Afterward, the glucose biosensor is biased with a voltage of 0.5 V and the resulting current is recorded over time for 200 s. Stand-alone (i.e. without needles) glucose biosensors (Fig. 3a-3) are characterized using same solutions and procedures, and used as reference to which microneedle-based biosensors are compared in terms of analytical parameters (i.e. accuracy, linearity, reproducibility, sensitivity, resolution). Experimental data on type#1 and type#2 microneedle-based biosensors and stand-alone biosensors, measured over the glucose concentration range 0–35 mM at different sampling times between 5 s and 200 s, both in ISF and PBS solutions, are summarized in Figs. S2, S3, and S4 (Supplementary materials). Fig. 3b shows calibration curves of type#1 microneedle-based glucose biosensors measured over the concentration range 0–35 mM in ISF solutions, at different sampling times between 5 s and 200 s. It is worth noting that, in chrono-amperometry the current (at a planar electrode) increases with analyte concentration and decays with

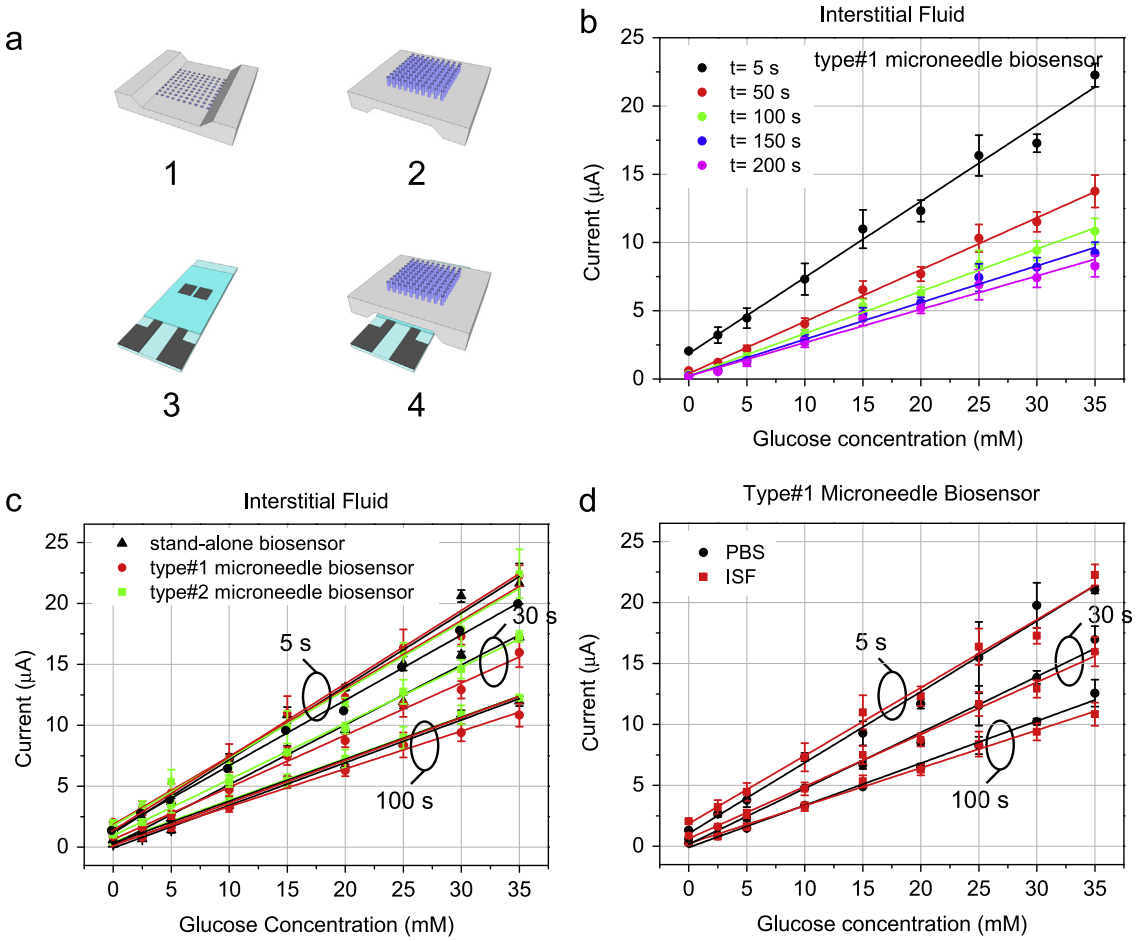

Fig. 3. Real-time glucose measurement by microneedle-based transdermal biosensors. (a) Schematic – front-side (1) and back-side (2) of the microneedle chip, stand-alone glucose biosensor (3) – of the microneedle-based biosensor (4) used for real-time glucose measurements by capillary-action. (b) Calibration curves (experimental data and linear regression) of type#1 microneedle-based glucose biosensors measured over the concentration range 0–35 mM in ISF solutions, at different sampling times between 5 s and 200 s. (c and d) Calibration curves (experimental data and linear regression) of (c) type#1 and type#2 microneedle-based glucose biosensors and stand-alone biosensors in ISF, and of (d) type#1 microneedle-based glucose biosensors both in ISF and PBS, measured over the concentration range 0–35 mM at sampling times of 5 s, 30 s, and 100 s.

time as given by the Cottrell equation, which explains why both current and sensitivity decrease as sampling time increases. Similar results are obtained both for type#2 microneedle-based glucose biosensors and for stand-alone glucose biosensors. Fig. 3c shows experimental data on type#1 and type#2 microneedle-based glucose biosensors superposed to those of the stand-alone biosensor, measured over the concentration range 0–35 mM in IFS solutions, for sampling times of 5 s, 30 s, and 100 s. Solid lines representing linear regression curves are superposed to experimental data both in Fig. 3b and c.

Performance of self-powered microneedle-based biosensors for glucose measurement in ISF results to be excellent, in terms of accuracy, linearity, reproducibility, sensitivity, and resolution, over the whole range of concentrations investigated and for any sampling time from 5 s to 200 s. For all the tested cases, control measurement with stand-alone biosensors yields analytical parameters that are in good agreement to those of microneedle-based biosensors.

Best performance (in terms of compromise between sensitivity, accuracy, and reproducibility) of microneedle-based glucose biosensors is achieved at sampling time of 30 s, for which type#1 (type#2) biosensor accuracy A is within $\pm 20\%$ of the actual glucose level for 96% (92%) of measures carried out on ISF solutions over the whole range 0–35 mM (0–630 mg/dl) of glucose concentrations. For comparison, 96% of measures have accuracy within $\pm 20\%$ for stand-alone biosensors, in ISF. Accuracy A is evaluated as error between measured and actual glucose concentrations. These values comply with current FDA standards, according to which above 75 mg/dl (4.2 mM), 95% measures must be within $\pm 20\%$ of the actual glucose level (International Organization for Standardization, 2003). As per FDA guidelines, further analytical parameters are evaluated at sampling time of 30 s (in ISF solutions over the whole range 0–35 mM of glucose concentrations) for both type#1 and type#2 microneedle-based biosensors, and compared to those of stand-alone biosensors. Linearity, which is evaluated in terms of squared correlation coefficient R^2 of the linear regression curves best-fitting experimental data, is 0.995 and 0.998 for type#1 and type#2 biosensors, respectively ($R^2=0.994$ for stand-alone biosensors). Reproducibility, which is evaluated in terms of coefficient of variations averaged over the whole range of glucose concentrations, $\%CV_{av}$, is 8.56% and 8.74% for type#1 and type#2 biosensors, respectively ($\%CV_{av}=6.55\%$ for stand-alone biosensors). Sensitivity S, which is evaluated in terms of slope of the linear regression curves best-fitting experimental data, is 0.43 μA/mM and 0.46 μA/mM for type#1 and type#2 biosensors, respectively ($S=0.49$ μA/mM for stand-alone biosensors). Resolution, which is evaluated in terms of limit-of-detection LoD, is 0.3 mM and 0.9 mM for type#1 and type#2 biosensors, respectively (LoD = 0.63 mM for stand-alone biosensors). Analytical parameters of microneedle-based biosensors at

Table 1
Analytical parameters of microneedle-based transdermal biosensors (best case). Comparison of the performance of microneedle-based transdermal biosensors and stand-alone biosensors at sampling time of 30 s, in terms of accuracy, linearity, reproducibility, sensitivity, and resolution, for glucose concentrations in the range 0–35 mM, both for ISF and PBS solutions.

	Type#1 micro-needle-based biosensor		Type#2 micro-needle-based biosensor		Stand-alone biosensor	
	ISF	PBS	ISF	PBS	ISF	PBS
Accuracy (*A*) (measures within $\pm 20\%$)	96%	92%	92%	96%	96%	99%
Linearity (R^2) ($0-35$ mM)	0.995	0.993	0.998	0.998	0.994	0.999
Reproducibility (%CV_{av})	8.56%	6.37%	8.74%	7.06%	6.55%	7.42%
Sensitivity (*S*) (μA/mM)	0.43	0.46	0.46	0.43	0.49	0.46
Resolution (LoD) (mM)	0.3	0.2	0.9	0.5	0.6	0.51

sampling time of 30 s (best case) are summarized in Table 1 both for ISF and PBS solutions, and compared to those of stand-alone biosensors.

Control experiments using PBS solutions (Fig. 3d) yield analytical parameters that are in good agreement with those obtained using ISF solutions, both for type#1 and type#2 microneedle-based glucose biosensors and for stand-alone biosensors, despite being ISF a more complex matrix with respect to PBS. Control experiments further validate high performance of glucose concentration measurements in ISF collected by capillary-action through microneedles, thus foreseeing future true pain-free measurement of glycaemia by microneedle-based transdermal biosensors.

4. Conclusions

In this work a self-powered pain-free microneedle-based transdermal biosensor for high-accuracy real-time measurement of glucose in ISF is demonstrated. Self-powered (pump-free) uptake of ISF is efficiently carried out with rate up to 1 μl/s by exploiting capillarity in tiny (borehole down to 4 μm) and densely-packed (up to 1×10^6 needles/cm^2) microneedles. By coupling the microneedles operating under capillary-action with an enzymatic glucose biosensor integrated on the back-side of the needle-chip, FDA-compliant in-vitro glucose measurement in ISF is performed with accuracy within $\pm 20\%$ of the actual glucose level for 96% of measures and coefficient of variation 8.56% in real-time (30 s) over the range 0–630 mg/dl, thus significantly improving microneedle-based biosensor performance with respect to the state-of-the-art.

Further work will be devoted to the investigation of in-vivo performance of the proposed self-powered microneedle-based biosensor, on the one hand, as well as to the integration of an enzyme-based biosensor right into the reservoir, on the other hand. As to the former, effective capillary uptake of ISF from skin will be investigated and lower potential values can be explored, with the aim of addressing possible clogging problems of microneedles and minimizing interference effects due to other chemical compounds, respectively; as to the latter, reduction of sample volume can be foreseen, which would be favorable in point-of-care applications.

This work envisages a novel class of minimally-invasive biosensors for point-of-care applications that (besides glucose concentration) would be employed to monitor parameters of clinical relevance in-situ, via transdermal route, through the use of ISF, with the advantage of eliminating discomfort due to needle pains and bypassing all the risks connected with blood extraction and manipulation, at the different levels.

Acknowledgment

Authors want to acknowledge Regione Toscana for partially funding this research activity within the project “A Minimally-Invasive Microsystem for Glucose Monitoring in Diabetic Patients” (CUP I51J11000010002).

Appendix A. Supplementary materials

Supplementary data associated with this article can be found in the online version at http://dx.doi.org/10.1016/j.bios.2014.11.010.

References

American Diabetes Association, 2010. Diabet. Care 33, S11.
Chen, C., Xie, Q., Yang, D., Xiao, H., Fu, Y., Tan, Y., Yao, S., 2013. RCS Adv. 3, 4473.
Collison, M.E., Stout, P.J., Glushko, T.S., Pokela, K.N., Mullins-Hirte, D.J., Racchini, J.R., Walter, M.A., Mecca, S.P., Rundquist, J., Allen, J.J., Hilgers, M.E., Hoegh, T.B., 1999. Clin. Chem. 45, 1665.
El-Laboudi, A., Oliver, N.S., Cass, A., Johnston, D., 2013. Diabet. Technol. Ther. 15, 101.
Fogh-Andersen, N., Altura, B.M., Altura, B.T., Siggaard-Andersen, O., 1995. Clin. Chem. 41, 1522.
Gilligan, B.C., Shults, M., Rhodes, R.K., Jacobs, P.G., Brauker, J.H., Pintar, T.J., Updike, S.J., 2004. Diabet. Technol. Ther. 6, 378.
Holman, R.R., Paul, S.K., Bethel, M.A., et al., 2008. N. Engl. J. Med. 359, 1577.
Hsu, C.-W., Wang, G.-J., 2014. Biosens. Bioelectron. 56, 204–209.
International Diabetes Federation, IDF Diabetes Atlas, sixth edition, 2013.
International Organization for Standardization. In: Vitro Diagnostic Test Systems—Requirements for Blood-glucose Monitoring Systems for Self-testing in Managing Diabetes Mellitus. DIN EN ISO 15197:2003.
Jang, H.D., Kim, S.K., Chang, H., Roh, K.-M., Choi, J.-W., Huang, J., 2012. Biosens. Bioelectron. 38, 184–188.
Kim, Y.-C., Park, J.-H., Prausnitz, M.R., 2012. Adv. Drug Deliv. Rev. 64, 1547.
Kitzmiller, J.L., Block, J.M., Brown, F.M., et al., 2008. Diabet. Care 31, 1060.
Joos P., 1999. Dynamic Surface Phenomena. In: VSP (Ed.). ISBN:9067643009, 9789067643009.
Lodwig, V., Kulzer, B., Schnell, O., Heinemann, L., 2014. J. Diabet. Sci. Technol. 0, 1.
Martin, S., Schneider, B., Heinemann, L., Lodwig, V., Kurth, H.-J., Kolb, H., Scherbaum, W.A., 2006. Diabetelogia 49, 271.
Miller, P.R., Skoog, S.A., Edwards, T.L., Lopez, D.M., Wheeler, D.R., Arango, D.C., Xiao, X., Brozik, S.M., Wang, J., Polsky, R., Narayan, R.J., 2012. Talanta 88, 739.
Mukerjee, E.V., Collins, S.D., Isseroff, R.R., Smith, R.L., 2004. Sens. Actuators A 114, 267.
Nathan, D.M., Cleary, P.A., Backlund, J.Y., et al., 2005. N. Engl. J. Med. 353, 2643.
Sakaguchi, K., Hirota, Y., Hashimoto, N., Ogawa, W., Sato, T., Okada, S., Hagino, K., Asakura, Y., Kikkawa, Y., Kojima, J., Maekawa, Y., Nakajima, H., 2012. Diabet. Technol. Ther. 14, 485.
Shlomowitz, M., Feher, D., 2014. Br. J. Diabet. Vasc. Dis. 14 (2), 60–63.
Stout, P.J., Peled, N., Erickson, B.J., Hilgers, M.E., Racchini, J.R., Hoegh, T.B., 2001. Diabet. Technol. Ther. 3, 81.
Strambini, L.M., Longo, A., Diligenti, A., Barillaro, G., 2012. Lab Chip 12, 3370.
Taguchi, M., Ptitsyn, A., McLamore, E.S., Claussen, J.C., 2014. J. Diabet. Sci. Technol. 8, 403.
Tamborlane, W.V., Beck, R.W., Bode, B.W., et al., 2008. N. Engl. J. Med. 359, 1464.
The Diabetes Control and Complications Trial Research Group, 1993. N. Engl. J. Med. 329, 977.
UK Prospective Diabetes Study (UKPDS) Group, 1998. Lancet 352, 837.
Vesper, H.W., Wang, P.M., Archibold, E., Prausnitz, M.R., Myers, G.L., 2006. Diabet. Technol. Ther 8, 76.
Wang, J., 2008. Chem. Rev. 108, 814–825.
Wang, P.M., Cornwell, M., Prausnitz, M.R., 2005. Diabet. Technol. Ther. 7, 131.
Yang, Z., Zhang, C., Zhang, J., Bai, W., 2014. Biosens. Bioelectron. 51, 268–273.
Zimmermann, S., Fienbork, D., Stoeber, B., Flounders, A.W., Liepmann, D., 2003. In: Proceedings of the Transducers, June 8–12, Boston, MA, USA.